JOURNAL OF AIRCRAFT
Vol. 43, No. 4, July–August 2006

Stochastic Analysis of a Nonlinear Aeroelastic Model Using the Response Surface Method

Peter J. Attar*
Computational Sciences Branch, Wright–Patterson Air Force Base, Ohio 45433-7913
and
Earl H. Dowell†
Duke University, Durham, North Carolina 27708

DOI: 10.2514/1.17525

An efficient method is presented for quantifying the effect of parametric uncertainty on the response of a nonlinear aeroelastic system. The proposal stochastic model uses a response surface method to map the random input parameters of the system to the specified system output (in this instance root-mean square wing tip response). To handle the bifurcation in the response surface due to aeroelastic self-excited instability, the response surface model is fit using a two region regression. The results from this model are compared to those from a full Monte Carlo simulation for both a one-dimensional random input parameter model (thickness) and a two-dimensional random input parameter model (thickness and modulus of elasticity). The response surface method results compare favorably with the full model results while achieving a 2 to 3 order of magnitude gain in computational efficiency.

Nomenclature

$[A_b]$	=	bound circulation influence coefficient matrix
$[A_w]$	=	wake circulation influence coefficient matrix
$A1_{im}, B1_{jm}, C1_{lom}$	=	coefficients in the x in-plane equations of motion
$A1_{in}, B2_{jn}, C2_{lon}$	=	coefficients in the y in-plane equations of motion
A_0, B_i, C_{ij}	=	constant coefficients in the response surface polynomial
a	=	parameter to be determined in the process of identifying the change line
$\bar{a}, \bar{b}, \bar{q}$	=	normalized (by the thickness) generalized coordinates
a_m	=	generalized coordinate in the x direction
b_o	=	generalized coordinate in the y direction
c	=	plate wave speed
c_{mean}	=	mean value for plate wave speed
E	=	plate elastic modulus
E_{mean}	=	mean value for plate elastic modulus
ET	=	interpolation matrix
f	=	function which maps input variables to the system response
$F(x, y, z, t)$	=	definition of wing solid boundary
h	=	nominal wing thickness
h_{mean}	=	mean value for plate thickness
$K1_{mlo}, K2_{nlo}, K3_{rsto}$	=	nonlinear coefficients in the out-of-plane equations of motion
mxy	=	number of modal functions used in the expansion of the in-plane displacements
n	=	number of random input variables
nxy	=	number of modal functions used in the expansion of the out-of-plane displacements
$P(x)$	=	standard Gaussian probability distribution
$p(x, y, t)$	=	pressure on wing surface
p_∞	=	freestream pressure
Q_0^P	=	nondimensional generalized aerodynamic loading
$\mathbf{q}$	=	relative velocity between the undisturbed fluid and wing
q_p	=	generalized coordinate in the z direction
r_i	=	random value drawn from standard Gaussian distribution
t	=	time
$\mathbf{U}_\infty$	=	freestream velocity of the wing
$u(x, y, t)$	=	plate deflection in the x (in-plane) direction
$v(x, y, t)$	=	plate deflection in the y (in-plane) direction
$w(x, y, t)$	=	plate deflection in the z (in-plane) direction
x, y, z	=	Cartesian coordinate
$\bar{x}, \bar{y}$	=	values of the random input parameters normalized by their respective mean values
x_i	=	ith random input variable
$\bar{x}_i$	=	mean value of ith random input variable
α	=	angle the freestream velocity makes with the undeformed wing
α_m	=	model functions used in the expansion of the x displacement
β_o	=	model functions used in the expansion of the y displacement
$\{\Gamma_b\}$	=	vector of bound circulation
$\{\Gamma_w\}$	=	vector of wake circulation
γ	=	system response modeled using response surface

Presented as Paper 2005-1986 at the 7th AIAA Non-Deterministic Approaches Forum, Austin, Texas, 18–21 April 2005; received 4 May 2005; accepted for publication 7 February 2006.

*NRC Fellow, Computational Sciences Branch, Air Force Research Laboratory; peter.attar@wpafb.af.mil. Member AIAA.

†William Holland Hall Professor, Department of Mechanical Engineering and Materials Science and Director of the Center for Nonlinear and Complex Systems. Dean Emeritus, Pratt School of Engineering, Honorary Fellow AIAA.

ϵ	=	quantity which represents variability not accounted for in f
$\xi_1, \xi_2, \ldots, \xi_n$	=	known input variables
ξ_o	=	σth modal damping
ρ_∞	=	freestream density
σ_i	=	uncertainty value for ith random input variable
τ	=	constant due to the nondimensionalization of the nonlinear plate equations
Φ	=	velocity potential
ϕ_p	=	modal functions used in the expansion of the z displacement
ω_o	=	σth model frequency
$\omega_{i,\text{mean}}$	=	mean value for ith model frequency

I. Introduction

COMPUTATIONAL methods in aeroelasticity alone are still not sufficient to assure system stability. Thus experiments and flight tests are extensively used to complement computational results, both of which are expensive. Flight tests can also be dangerous and put both the aircraft and the pilot at risk. The reluctance to rely more heavily on computational methods is due to three perceived uncertainties:

1) Uncertainties in the physics of the mathematical model. Are the actual equations used to model the physics of the problem correct? For example, in a Navier–Stokes simulation, what turbulence model should be used to capture the correct physics of the problem? Proper boundary and initial conditions are other examples of uncertainty

2) Uncertainty in the solution method. Is the numerical method converged with respect to discretization, in both time and space? How does one know how many data points are needed when a convergence study is performed?

3) Uncertainty in the physical parameters of the problem. In classical deterministic methods, physical parameters such as flow density, structural modulus of elasticity, etc. are assumed to be known. However in reality there is always an uncertainty in these quantities. All three of these uncertainties arise when dealing with problems in aeroelasticity. When nonlinearities are involved these become even more problematic since some forms of nonlinearities have a destabilizing effect.

Recently research dealing with stochastic analysis methods in aeroelasticity has been undertaken to better quantify uncertainty in aeroelastic computational models. Classically stochastic analyses in computational aeroelasticity have used Monte Carlo simulation (MCS) on the governing equations of motion to quantify input uncertainty and to estimate system response probability density functions. In this paper this method will be referred to as the classical MCS method. Although this method is the most accurate means of performing a stochastic analysis, it is extremely expensive computationally because the full aeroelastic system of equations must be solved for each realization of the random input parameters. Approximate methods which reduce the computational time are needed to make stochastic analysis feasible for use in design.

Two approximate methods which are often used to quantify uncertainty are first-order and second-order reliability methods [1]. Because these methods use local expansions (about a specified design point) in the random variables they often do not work well for highly nonlinear systems. Reduced-order modeling (ROM) [2] can also be used because the end result of such modeling is a smaller, lower dimensional system of equations which capture all of the important dynamics of the original full system. These lower dimensional systems of equations can then be used in a MCS simulation. Two possible drawbacks of some ROM methods are 1) oftentimes many solutions of the full system of equations are needed to be able to form an accurate reduced-order model and 2) the reduced-order model may not be robust with respect to change of the input parameters.

An active area of research is one which combines stochastic spectral projection methods with computational aeroelasticity models. In stochastic spectral projection, the output variables (for example, pitch and plunge response) are written as a series expansion of time dependent coefficients and a specified basis which is a function of the random input variables. Historically polynomial functions have been chosen for the basis. This method is referred to polynomial chaos expansion (PCE) [3,4]. The main drawback of PCE is the number of terms in the expansion needed to give a converged result for problems which have more than one input parameter. Millman et al. [5] have recently used a basis which consists of trigonometric functions (Fourier basis). Whereas in their paper they show this expansion to be more efficient than PCE due to faster convergence of the series expansion, the method requires access to the original full set of equations so that they can be modified. This limits the method to situations where the source code for the solvers is available, which is often not the case if one is using a commercial software package. Also even if one has access to the equations, transforming the original equations is a nontrivial task for complicated systems. In an effort to overcome the difficulties associated with intrusive stochastic methods, Millman and his colleagues have recently employed [6] a nonintrusive stochastic projection method to predict the effects of uncertainty on nonlinear systems. In this work the authors use B splines as a way of dealing with the piecewise continuous projections which arise due to bifurcation in the aeroelastic system.

In other recent work in uncertainty analysis for nonlinear aeroelastic models, Beran and Pettit used polynomial chaos expansions, in both an intrusive and a nonintrusive manner, to obtain spectral representations of stochastic system response for a two-dimensional airfoil section in incompressible flow. The nonlinear behavior for this airfoil was modeled using nonlinear spring stiffness terms. The nonintrusive method was found to be both accurate and highly efficient.

Lindsley et al. [7] examined the effect of uncertainty in elastic modulus and boundary conditions on the aeroelastic response of a nonlinear panel in supersonic flow. In this work the panel was modeled structurally using the von Karman plate equations and the flow is modeled using piston theory aerodynamics. Probabilistic response distributions were obtained through classical Monte Carlo simulation.

For an excellent review of the current state of the art in uncertainty analysis as it applies to aeroelasticity see the review paper by Pettit [8].

In this paper a response surface method will be used to generate empirical density functions. The response surface method has been used in stochastic finite element analysis of structural systems [9]. In the response surface method, the output quantity to be studied is written as a polynomial in the set of random input variables. The unknown coefficients of the polynomial are then found using regression analysis. The number of classical MCS which must be run is then of the same order of magnitude as the number of terms in the polynomial.

In the work which will be presented here, the response surface methodology will be used to predict probability density functions of the rms displacement for a delta wing aeroelastic model undergoing limit cycle oscillations (LCO). The thickness and modulus of elasticity will be used as the stochastic input variables. To deal with the discontinuity in the response surface due to bifurcation, a two region regression analysis will be used. The computational aeroelastic model used to compute the response in the analysis is one which combines a linear vortex lattice aerodynamic model with a nonlinear von Karman plate model. Stochastic results computed using this model will be compared to those from a traditional MCS.

II. Theory

A. Response Surface Methodology

The response surface methodology is used extensively by researchers in many different technical fields for situations where several input parameters may influence the response of a system. In engineering it is often used in structural reliability analysis to approximate a limit state function. The basic idea behind the

response surface method is to represent some output measure as a function of known input variables. In general the response of a system γ can be written in the following manner:

$$\gamma = f(\xi_1, \xi_2, \ldots, \xi_n) + \epsilon \tag{1}$$

In Eq. (1) the ϵ is a quantity which accounts for other types of variability not accounted for in f. Here it is assumed to have a normal distribution and zero mean and therefore is not considered in the analysis.

Often times the true form of f is unknown and/or very complicated. In these cases a form must be chosen. The usual manner in which this is done is to assume some low-order polynomial form for the function. In the work presented here a second-order polynomial will be used. The full second-order model can be written in the following manner:

$$\gamma = A_1 + \sum_{i=1}^{n} B_i \xi_i + \sum_{i=1}^{n} \sum_{j=i}^{n} C_{ij} \xi_i \xi_j \tag{2}$$

where A_0, B_i, and C_{ij} are constant coefficients which are found using a least-squares method and a limited number of classical MCS, and n is the number of random input variables to be modeled. The values for the output y computed using the classical MCS are then used, along with the corresponding inputs ξ_i, in a least-squares analysis to find the coefficients in Eq. (2).

When modeling aeroelastic systems using stochastic methods, both subcritical and supercritical bifurcation may occur. This bifurcation of the output variable causes the response surface to have a discontinuity which often produces large errors when one uses a "one region" regression. Figure 1 is a plot of the rms tip response of a flat plate delta wing (output variable) as a function of thickness (input variable). Shown on the plot are the rms response values of the full Monte Carlo simulation (circles) and the fitted response surface/line from a regression which uses a one region regression and a regression which uses a two region regression. The two region model will be explained next.

In the current work the discontinuity in the response surface due to bifurcation is modeled using a two region model. This model was implemented for a one-dimensional or two-dimensional input parameter space. Curves or surfaces are fit in two regions which are separated by a change-point value (for a one-dimensional input parameter space) or change line (for a two-dimensional input parameter space). See Fig. 2 for a schematic of the change point/change line idea. In the discussion to follow, the term change point will be used for both one- and two-dimensional random input parameter spaces.

Since it is unlikely that one of the classical MCS will be run with an input parameter realization which lies at a change point, the change point of the response surface must be approximated. This can be accomplished by either extrapolation or using a method which assumes a change point and then fits a response surface using this information. The sum of the squares error is then calculated for the response surface. Multiple change points are considered and the one which results in a response surface which has the smallest least-squares error is used as the change point. This change point is then used to separate the two response surface regions when this surface is employed to generate the output.

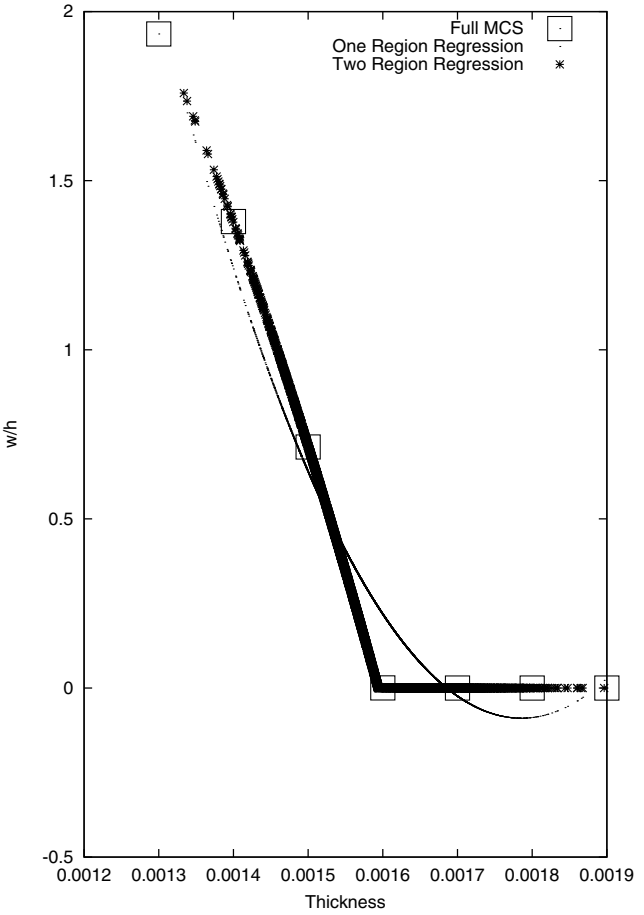

Fig. 1 Regression analysis for a response surface with a discontinuity: comparison of a two region fit and a one region fit.

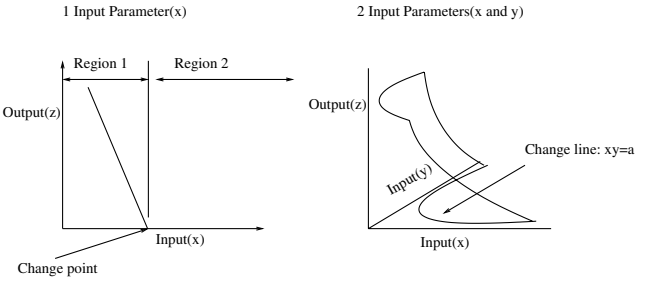

Fig. 2 Illustration of the change point/change line idea.

B. Aeroelastic Modeling

An abbreviated discussion of the aeroelastic model is presented here. For more detail, see [10–12].

1. *Structural Model*

The delta wing structure used in this study is modeled as a thin plate. The structural theory used is the dynamic version of the nonlinear plate equations attributed to von Karman. It includes higher order terms in the strain-displacement relations and does not include transverse shearing effects. The kinetic and strain energies are expressed in terms of modal expansions of the in-plane and out-of-plane plate deflections. Finally Lagrange's equations are used to derive equations for the modal coordinates. In the strain and kinetic energies the in-plane inertia terms have been neglected and the plate is assumed to have a constant (though uncertain) thickness h.

The plate deflections in the out-of-plane and in-plane directions can be represented as

$$u(x, y, t) = \sum_{m} a_m(t) \alpha_m(x, y) \qquad m = 1 \cdots mxy \tag{3}$$

$$v(x, y, t) = \sum_{o} b_o(t) \beta_o(x, y) \qquad o = 1 \cdots mxy \tag{4}$$

$$w(x, y, t) = \sum_{p} q_p(t) \phi_p(x, y) \qquad p = 1 \cdots nxy \tag{5}$$

where the modal functions α, β, and ϕ are calculated using the commercial finite element package ANSYS [13]. The finite element model which is used to calculate the modal functions contains 900

elements. The element used is a 4 node shell element. To determine the out-of-plane and in-plane modal functions the model is fully constrained along a partial portion of the root chord and allowed to displace and rotate freely at all other portions of the wing.

The in-plane equations of motion can be found by placing the modal expansions in Eqs. (3–5) into the strain energy expression and then using Lagrange's equation. Note that all of the aerodynamic loading is assumed to occur in the out-of-plane direction. The nondimensional in-plane equations of motion become a_m:

$$\sum_i \bar{a}_i A1_{im} + \sum_j \bar{b}_j B1_{jm} = \sum_l \sum_o \bar{q}_l \bar{q}_o C1_{lom} \tag{6}$$

b_n:

$$\sum_i \bar{a}_i A2_{in} + \sum_j \bar{b}_j B2_{jn} = \sum_l \sum_o \bar{q}_l \bar{q}_o C2_{lon} \tag{7}$$

Similarly the nondimensional out-of-plane equations of motion become

$$\ddot{\bar{q}}_o + 2\xi_o \omega_o \dot{\bar{q}}_o + \omega_o^2 \bar{q}_o + \tau\left(\sum_m \sum_l \bar{a}_m \bar{q}_l K1_{mlo} + \sum_n \sum_l \bar{b}_n \bar{q}_l K2_{nlo} + \sum_r \sum_s \sum_t \bar{q}_r \bar{q}_s \bar{q}_t K3_{rsto}\right) + \bar{Q}_o^P = 0 \tag{8}$$

where in the above equations the coefficients multiplying the modal coordinates depend upon the modal functions (see [10] for details). In the equations above the spatial coordinates x, y, and z are normalized by the root chord dimension whereas the displacements u, v, and w are normalized by the plate thickness h.

2. Aerodynamic Modeling

The flow field about the delta wing model is assumed to be a potential flow. Therefore the equations of motion for the fluid can be reduced to Laplace's equation

$$\nabla^2 \Phi = 0 \tag{9}$$

The boundary conditions which must be satisfied are that of zero normal flow on the wing:

$$[\nabla \Phi + \mathbf{q}(\mathbf{x}, \mathbf{y})] \cdot \mathbf{n}(\mathbf{x}, \mathbf{y}) = 0 \tag{10}$$

and also that the disturbance created by the potential must decay at distances far from the wing. The latter condition can be expressed as

$$\lim_{r \to \infty} \nabla \Phi = 0 \tag{11}$$

where $\mathbf{q}$ is the relative velocity between the undisturbed fluid in the fluid domain and the wing. Using Green's identity it can be shown [14] that a solution to Eq. (9) can be found by distributing elementary solutions to Laplace's equation on the problem boundaries. For the model presented here this is accomplished by distributing vortex rings on the wing surface and in the wake.

If the solid boundary of the wing is defined as

$$F(x, y, z, t) = z - \eta(x, y, t) = 0 \tag{12}$$

then the zero normal flow boundary condition, Eq. (10), can be expressed as

$$\frac{DF}{Dt} = \frac{\partial F}{\partial t} - \mathbf{U}_\infty \cdot \nabla F + \nabla \Phi \cdot \nabla F = 0 \tag{13}$$

where $\mathbf{U}_\infty$ is the freestream velocity of the wing as viewed from the inertial frame.

If the small disturbance approximation to the aerodynamic boundary condition is used along with Eq. (15), Eq. (13) can be rewritten in the following form:

$$\frac{\partial \Phi}{\partial z} = \mathbf{U}_\infty\left(\alpha - \frac{\partial \eta}{\partial x}\right) + \frac{\partial \eta}{\partial t} \tag{14}$$

where the angle α is the angle the freestream velocity $\mathbf{U}_\infty$ makes with the undeformed wing.

For the thin surface with zero initial curvature considered here, $\eta(x, y, t)$ is the out-of-plane structural deformation of the surface

$$\eta(x, y, t) = \sum_p q_p(t) \phi_p(x, y) \qquad p = 1 \cdots nxy \tag{15}$$

The flow model is solved by placing vortex rings on the wing and in the wake [11,15–17]. The wake is assumed to be planar so that the force-free wake condition is not imposed. This is usually a valid assumption for simulations involving the translation of a fixed wing and using this assumption dramatically increases the computational efficiency of the model.

If Eq. (15) is used together with Eq. (14), the resulting zero normal flow boundary condition equation can be expressed in matrix form as

$$[A_b]\{\Gamma_b\}^{n+1} = [ET][\phi]\left\{\frac{\partial q}{\partial t}\right\}^{n+1/2} + \mathbf{U}_\infty [ET]\left[\frac{\partial \phi}{\partial x}\right]\{q\}^{n+1/2} + \mathbf{U}_\infty\{\alpha\} - [A_w]\{\Gamma_w\}^n \tag{16}$$

where $[A_b]$ is the influence coefficient matrix for the influence of the wing bound circulation at the wing collocation points, $[A_w]$ is the influence coefficient matrix for the influence of the wake circulation at the wing collocation points, and $\{\Gamma_b\}$ and $\{\Gamma_w\}$ are the vectors of bound and wake circulation, respectively. Also the superscripts n, $n + 1/2$ and $n + 1$ represent the time steps in the time integration where $n + 1/2$ represents an intermediate step during the fluid-structure subiteration. Finally ET is a matrix which interpolates the displacements w from the structural model nodes to the aerodynamic model collocation points. This interpolation is done with a thin-plate spline. See Katz and Plotkin [18] for details on the use of vortex rings to discretize the flow model.

The pressure on the wing is computed using the unsteady form of Bernoulli's equation:

$$\frac{p_\infty - p}{\rho_\infty} = \frac{(\nabla \Phi)^2}{2} - \left(\mathbf{U}_\infty + \frac{\partial w}{\partial t}\right) \cdot \nabla \Phi + \frac{\partial \Phi}{\partial t} \tag{17}$$

3. Fluid-Structure Coupling

To model the aeroelastic phenomena, the structural model and aerodynamic model must be coupled. In the out-of-plane structural equations of motion, (9), this coupling is due to the generalized force due to pressure $\bar{Q}_o^P$. In the aerodynamic system, the coupling occurs through the zero through flow aerodynamic boundary condition equation (16).

The structural equation of motion is integrated forward in time using a Hamming predictor-corrector scheme [19]. Because the fluid and structure are loosely coupled a subiteration strategy is used to reduce the lag errors incurred by not solving the fluid and structure simultaneously.

III. Computational Procedure

In the work presented in this paper, the root-mean square tip response of a 45 deg delta wing is studied using both a one-dimensional and two-dimensional random input parameter space. The random deviates of the random input variables are generated using a pseudorandom number generator. The random variables are assumed to have a Gaussian probability distribution with zero mean and a standard deviation of 1 which can be represented in the following manner:

$$P(x) = \frac{1}{\sqrt{2\pi}} \exp\left[\frac{-x^2}{2}\right] \tag{18}$$

The random deviates are generated using a method suggested by Box

and Müller [20]. The effects of uncertainty in the random input variables are simulated by smearing the data points. If the chosen random input variable has a mean of $\bar{x}_i$ and uncertainty σ_i and Gaussian uncertainties are assumed, the smear value of the input variable x_i can be written as

$$x_i = \bar{x}_i + \sigma_i r_i \tag{19}$$

where r_i is a random variable drawn from the standard Gaussian distribution with mean of 0 and a standard deviation of 1.

The two input variables which are assumed to have random distributions are chosen to be thickness and modulus of elasticity. The mean value for the thickness is chosen to be $0.0016m$ and the uncertainty is taken to be $0.00008m$. The mean value for the modulus of elasticity is taken to be 3.3×10^9 Pa and the uncertainty value is taken to be 3.3×10^8 Pa.

Since the modes of the structure used in the Rayleigh–Ritz solution are computed before the simulation is run, the modal frequencies must be updated for each new value of the random input values. In this work the thickness and elastic modulus are not functions of x, y, or z, so the eigenvectors are assumed to not change with small deviations in thickness or modulus of elasticity. The structural modal frequencies ω_i are updated using the following relationships:

$$c^2_{\text{mean}} = \frac{E_{\text{mean}} h^3_{\text{mean}}}{[12(1-\nu^2)]\rho h_{\text{mean}}} \tag{20}$$

$$c^2 = \frac{Eh^3}{[12(1-\nu^2)]\rho h} \tag{21}$$

$$\omega_i = \omega_{i,\text{mean}} \frac{c}{c_{\text{mean}}} \tag{22}$$

The values of c, E, h, and ω_i are the current values of these quantities.

Note that if the thickness and modulus of elasticity were instead considered to be random functions of x and y, a first attempt at modeling this could include considering the mode shapes themselves to be random variables. This would allow the analyst the ability to consider these variations to be considered without the need to go back to the original finite element model.

An algorithm is now presented for the calculation of response surface models using the two region regression idea:

Step 1: Choose N values for the random input parameters which will be used to train the response surface model. This can be done by "inspection," as was done is this work, or by a method such as central composite design (CCD) [21]. As the random input parameter space increases methods such as CCD should probably be used. The number of training points chosen N should be at least as large as the number of coefficients in the response surface model. In the work presented here eight training points were used for the case where there was one random input parameter. Fifteen training points were used for the case which had two random input parameters.

Step 2: Choose the output value at which the response surface will have a discontinuity. For the rms tip response studied here, this value was taken to be a small nonzero value.

Step 3: Choose the order of the response surface model to be used. In the work presented here a quadratic model with cross terms present (for the two-dimensional model) was used.

Step 4: Using the values of the random input parameters chosen in step 1, run N separate simulations which solve the aeroelastic equations of motion, Eqs. (6–9) and (16), for the output parameter, which in this case is the rms tip deflection of the wing. Note that if a parallel processing capability were to be implemented, this step would be "perfectly parallel" since each separate processor could be used to run a simulation with a given input parameter with no need for communication with other processors.

Step 5: Using the value chosen in step 2 and the results from step 4, determine how many training points lie in each of the two regions of the response surface.

Step 6: Determine the relevant characteristics of the change point/change line. For the one-dimensional parameter space the value of the change point is determined by choosing values of the random input parameter between the maximum and the minimum as specified in step 1 and then adding this value to the array of training points. By definition at the change point the value of the output parameter is equal to the value chosen in step 2, and so this value is added to the array of output values calculated in step 4. With these data the response surface for region 1 is fit and the least-squares error calculated. Another value of the input parameter is then chosen and this process is repeated. The value of the input parameter which gives the smallest least-squares error is then chosen as the change point and the resulting coefficients [A_0, B_i, and C_{ij} from Eq. (2)] of the response surface model are chosen as the ones to be used in further analysis.

For the two-dimensional input parameter space used here (thickness and elastic modulus are the random parameters), the change line was chosen to be a hyperbola with equal major and minor axes and rotated 45 deg

$$\tilde{x}\,\tilde{y} = a^2 \tag{23}$$

where $\tilde{x}$ and $\tilde{y}$ are the values of the random input parameters normalized by their respective mean values. To determine the value of a, a procedure similar to the one above was used where values of a were chosen and then used in a least-squares analysis.

Step 7: Now that the equations for the response surfaces in the two regions have been determined, they can be used to generate the values of the output parameter for random deviates of the random input parameters generated using Eqs. (18) and (19). Note that the only calculation which must be performed to generate the output parameter data using the response surface is an evaluation of Eq. (2).

IV. Results

In the work presented here a statistical analysis of the normalized (by the thickness) rms tip amplitude of a 45 deg, Plexiglas delta wing is studied using both a classical MCS and a reduced-order response surface method. The statistical analysis was conducted for both one-dimensional and two-dimensional random parameter spaces. For the cases with only one random input parameter, this parameter was chosen to be the thickness. For the cases which had two random input parameters both the thickness and the modulus of elasticity was chosen.

For the classical MCS the delta wing response was integrated forward in time for 2 s of simulation "time" t. In the work presented here the rms normalized tip response was used as the output parameter γ in Eq. (2). This rms value was calculated using the last 25% of the time history data. Note that other quantities could have been used in place of the rms tip response. In theory quantities which are time dependent could be used in the method. However doing so would dramatically increase the number of Monte Carlo simulations which would need to be run to build the response surface model. A possible solution to this problem would be the use of spectral in time methods [22–27] in combination with the response surface methodology presented here.

Three out-of-plane modes and 10 in-plane modes were used in the structural model. The aerodynamic model contained 100 bound vortex rings and 3 chords of wake were kept. Note that this aeroelastic model was chosen for speed rather than accuracy. In reality for the structural model to give good quantitative results at least 10 out-of-plane modes should be kept and at least 50 in-plane modes should be used. However as will be reported later, even with this reduced size aeroelastic model, a full ensemble of realizations using the classical MCS took a number of days to complete.

Figure 3 shows the rms response as a function of the random parameter (thickness) for three separate flow velocities, $\mathbf{U}_\infty = 23$, 27, and 31 m/s. A total of 5000 realizations are shown for each flow velocity in Fig. 3, with eight of those solved for directly using the aeroelastic equations of motion. These eight realizations were then used to generate the response surface using the method described

previously. Note that from Fig. 3 it appears that in region 1 the output parameter is a weak nonlinear function of the thickness.

In Figs. 4–6 the output parameter is plotted versus the two-dimensional random input parameter space for flow velocities of 23, 27, and 31 m/s. Once again 5000 realizations are shown in each of the figures with 15 of those solved for using the aeroelastic equations of motion. Note that a deterministic analysis would result in only one realization (one point) on each of Figs. 4–6.

In Figs. 7–11, estimates are given for the probability that a response will have a given rms amplitude for a specified flow velocity. Five such flow velocities were used in this analysis: 23, 25, 27, 29, and 31 m/s. The figures show both the statistical data determined using realizations calculated using the classical MCS and the statistical data determined using realizations computed with the response surface method. Also shown on these figures are the deterministic responses, which correspond to the rms response calculated using the aeroelastic model with the mean value for the thickness. Note that in Figs. 7 and 8, which are for velocities below the deterministic flutter speed, both the full method and the response surface method predict small nonzero probabilities that an LCO will occur at these speeds whereas a purely deterministic analysis would predict a zero response. In Figs. 9–11 the largest probabilities for nonzero response occur at the deterministic value of the rms response. For Figs. 9 and 10 the probabilities calculated using the response surface method match very well with those computed using the classical MCS. In Fig. 11 the response surface method predicts a slightly larger spread in the response data than does the full MCS.

Although the results using both the classical MCS and the reduced-order response surface method compare favorably, the total computational time needed to run the classical MCS for 5000 realizations at each velocity was greater by almost a factor of 10^3 than was needed by the response surface method. Almost 6 days of computational time was needed to run the full model while only 11 min were needed to run the response surface models. Although 6 days may still be a reasonable amount of time to wait for the statistical results reported here, note that, as was stated previously, this aeroelastic model was set up for speed rather than accuracy. If,

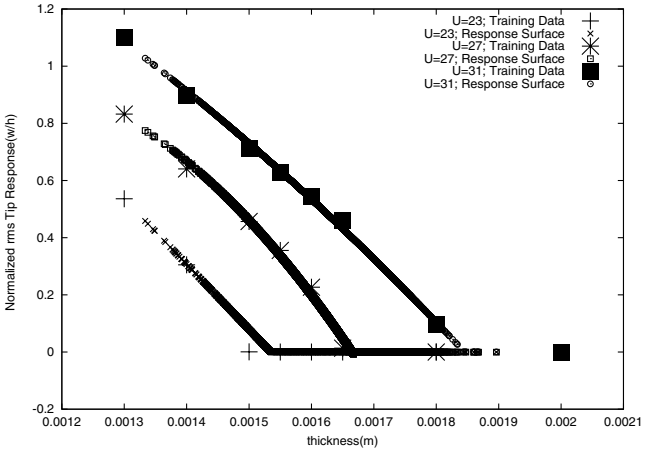

Fig. 3 rms amplitude versus random variable thickness.

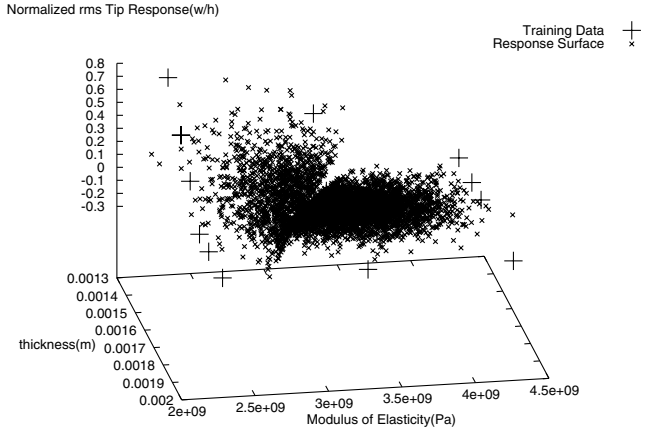

Fig. 4 rms amplitude plotted as a function of the two-dimensional random parameter space for a flow velocity of 23 m/s.

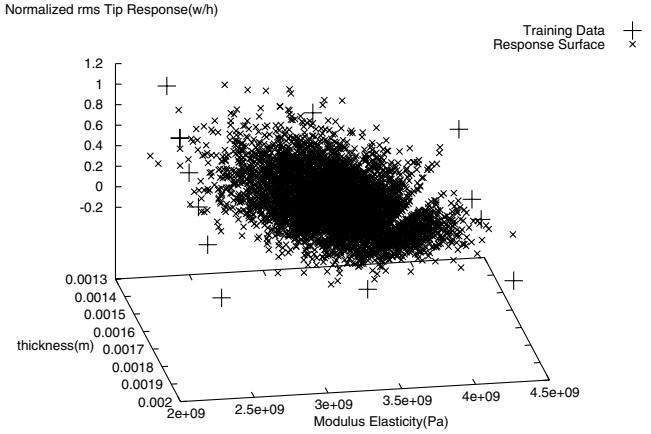

Fig. 5 rms amplitude plotted as a function of the two-dimensional random parameter space for a flow velocity of 27 m/s.

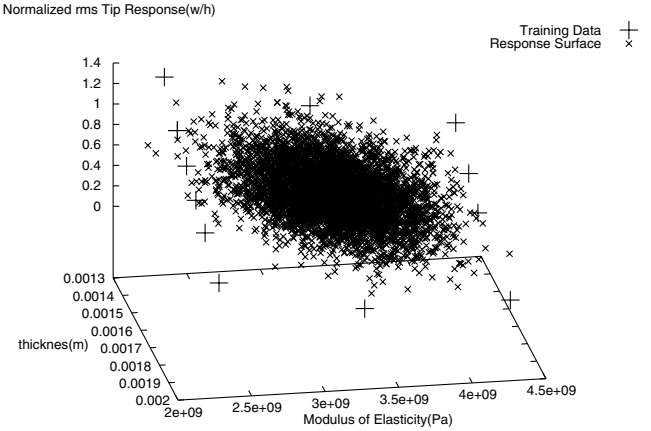

Fig. 6 rms amplitude plotted as a function of the two-dimensional random parameter space for a flow velocity of 31 m/s.

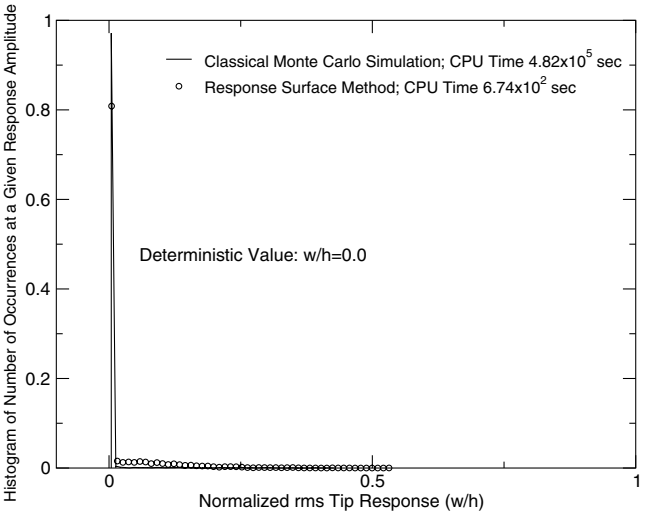

Fig. 7 Probability of rms response for a flow velocity of 23 m/s. The realizations were generated for a one-dimensional random parameter space.

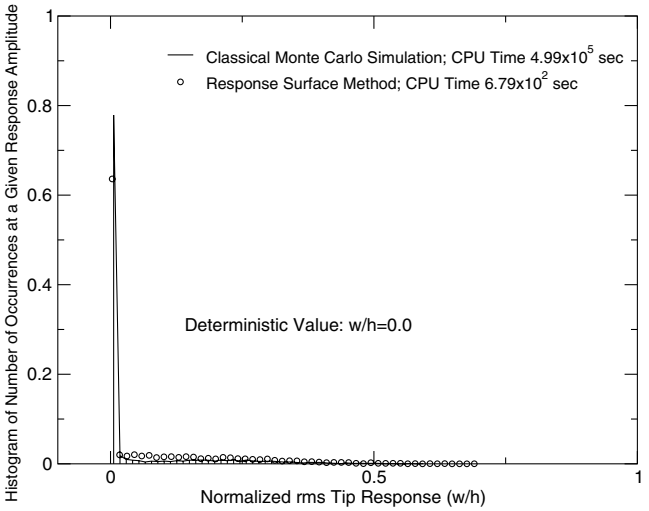

Fig. 8 Probability of rms response for a flow velocity of 25 m/s. The realizations were generated for a one-dimensional random parameter space.

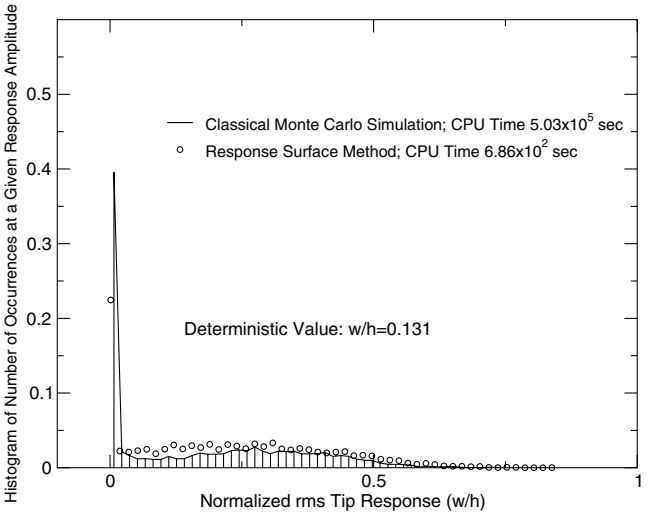

Fig. 9 Probability of rms response for a flow velocity of 27 m/s. The realizations were generated for a one-dimensional random parameter space.

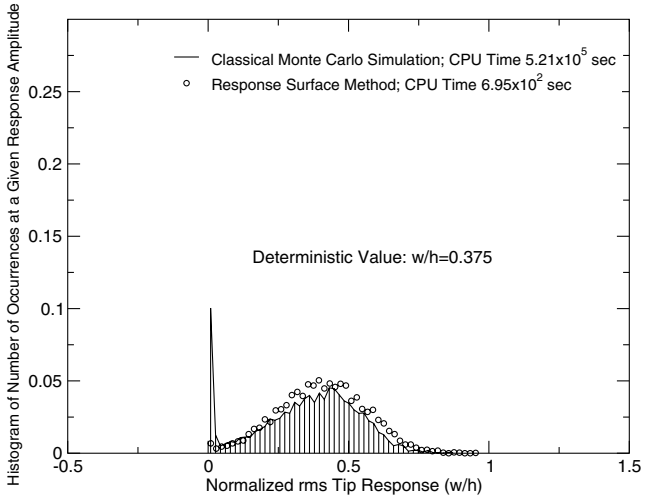

Fig. 10 Probability of rms response for a flow velocity of 29 m/s. The realizations were generated for a one-dimensional random parameter space.

for example, the high fidelity aeroelastic model used in [17] was used in place of the current aeroelastic model the time to run 5000 realizations of the classical MCS would increase from 6 days to over 8400 days while the response surface method used here would take approximately 13 days to run. Clearly running a classical Monte Carlo simulation would not be possible here.

Figures 12–16 are plots of the estimated probabilities of response for five different flow velocities. The realizations here were generated for two random parameters, thickness and modulus of elasticity. Once again when compared to the classical MCS, the response surface method appears to do a reasonable job of predicting the response probabilities. For the two-dimensional random parameter case shown in Figs. 12–16, the response surface method appears to improve as the flow velocity increases with the lower flow velocity results showing the largest errors at the nonzero amplitude peaks in the probabilities. Note that the negative rms values reported in Figs. 12–15 are due to errors in the curve fit for region 1 of the response surface. For the current work it is possible to just prescribe a zero output value for realizations determined to be in region 1. However to keep the method as general as possible the response surface for region 1 was actually a curve fit. These errors could also be reduced by increasing the integration time for the Monte Carlo

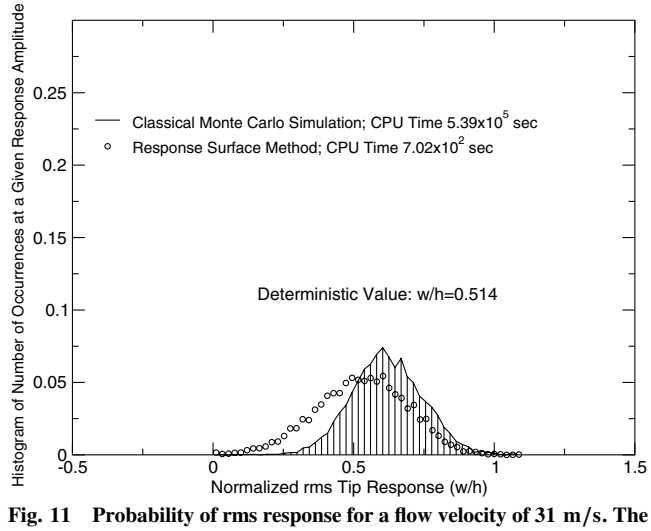

Fig. 11 Probability of rms response for a flow velocity of 31 m/s. The realizations were generated for a one-dimensional random parameter space.

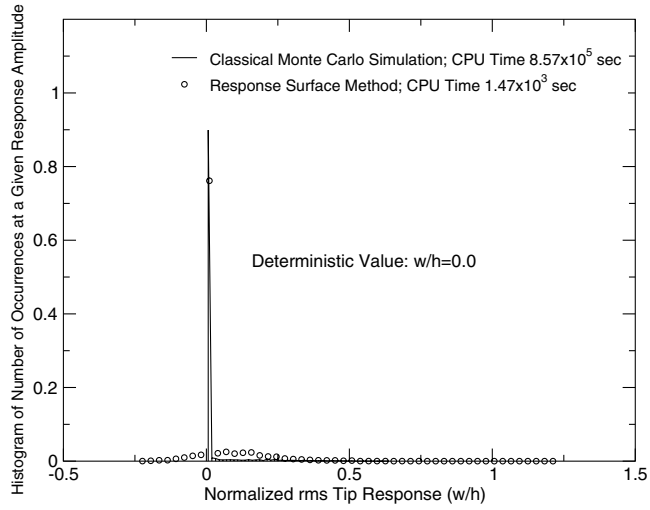

Fig. 12 Approximate probability of rms response for a flow velocity of 23 m/s. The realizations were generated for a two-dimensional random input parameter space.

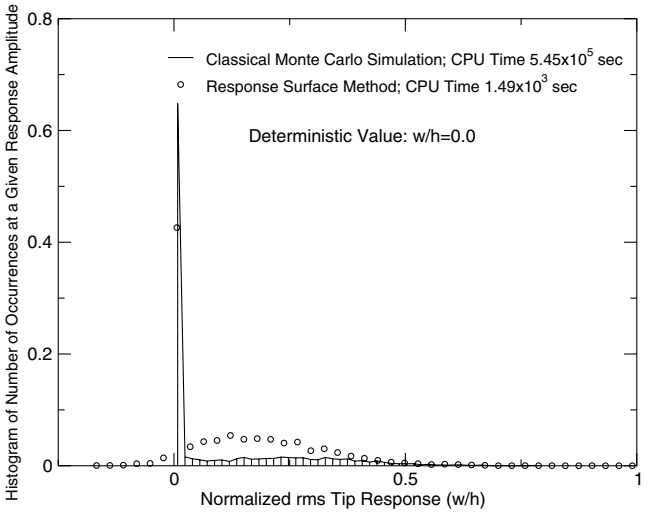

Fig. 13 Approximate probability of rms response for a flow velocity of 25 m/s. The realizations were generated for a two-dimensional random input parameter space.

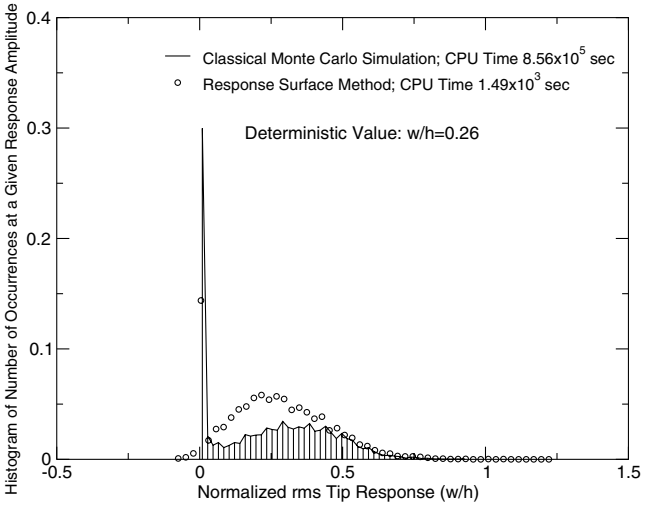

Fig. 14 Approximate probability of rms response for a flow velocity of 27 m/s. The realizations were generated for a two-dimensional random input parameter space.

simulation of the governing aeroelastic equations used to fit the response surface. This would have given output values which were closer to zero and the resulting regression would have been more accurate. Another option for reducing this error would be to use a different function (i.e., something other than a second-order polynomial) to represent the response surface.

Figure 17 is a plot of the probability of the rms tip response exceeding $w/h = 0.5$ as a function of the flow velocity. Shown on this plot are the classical MCS results and the response surface model results for both the one- and two-dimensional random input parameter cases. The value of $w/h = 0.5$ has no specific relevance but was chosen because it was a response value which was greater than the deterministic values for all but the highest flow velocity. So if only a deterministic analysis were to be performed here, the probability of "failure" would be zero all the way up to a flow velocity of 31 m/s and then it would be 1. With the stochastic analysis the probability of failure has a nonzero value at a flow velocity as low as 25 m/s. In comparing the classical MCS to the response surface model, the response surface results show good correlation with the full model for most of the data points. Only at a flow velocity of 31 m/s, and only for the one random parameter case, do the response surface results show a significant error when compared to the classical MCS results. The error for this one data

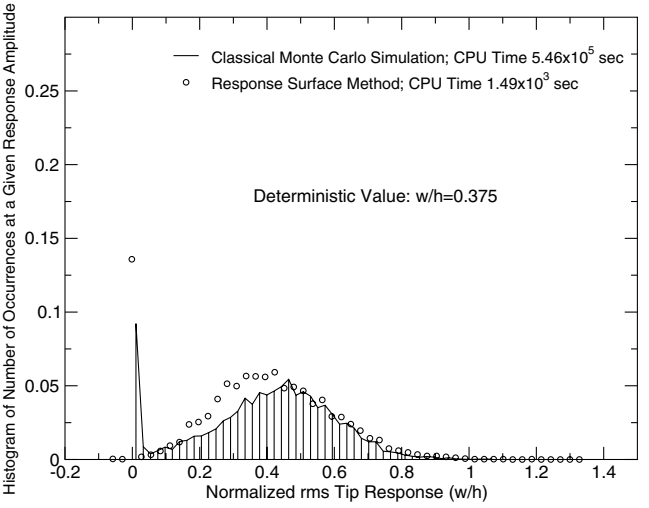

Fig. 15 Approximate probability of rms response for a flow velocity of 29 m/s. The realizations were generated for a two-dimensional random input parameter space.

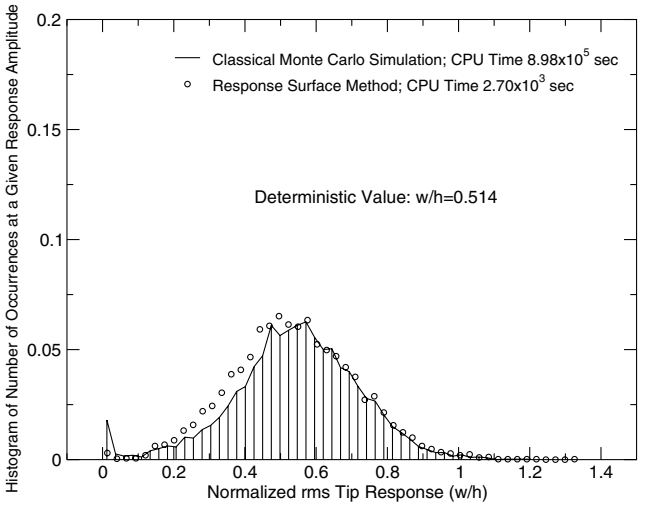

Fig. 16 Approximate probability of rms response for a flow velocity of 31 m/s. The realizations were generated for a two-dimensional random input parameter space.

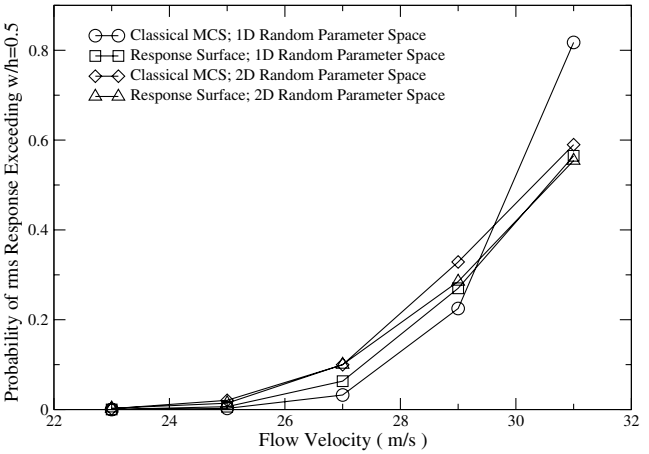

Fig. 17 A plot of the probability that a tip response will exceed $w/h = 0.5$ for a given flow velocity. Shown on the plot are the classical Monte Carlo results and response surface results for both the one and two random parameter cases.

point is due to the excessive spread in the response data predicted by the response surface method (see Fig. 11).

V. Conclusion

A computationally efficient response surface method for determining the effect of parametric uncertainties has been presented. The method was applied to a nonlinear aeroelastic system which consisted of a delta wing in low subsonic flow modeled using a nonlinear structural model and a linear aerodynamic model. The effects of both one-dimensional (thickness) and two-dimensional (thickness and elastic modulus) random parameter spaces on the specified output parameter (rms wing tip response) were considered. To better model the bifurcation in the response surface due to aeroelastic instabilities, a two region regression was used to fit the parameters needed for the response surface model. The results of the response surface method were compared to those computed using a Monte Carlo simulation on the governing aeroelastic equations of motion (classical MCS) and showed generally good correlation with the classical MCS while achieving 2–3 orders of magnitude greater computational efficiency. Further work could include representing the response surface using other types of functions and also the use of a higher fidelity aeroelastic model to generate sampling data for construction of the response surface model.

Acknowledgements

This work was supported under an AFOSR grant "A Study of Uncertainties in Nonlinear Aeroelastic Systems." The authors would like to thank Clark Allred for his advice and support.

References

[1] Melchers, R. E., *Structural Reliability Analysis and Prediction*, 2nd ed., Wiley, New York, 1999.

[2] Dowell, E., Hall, K., Thomas, J., Florea, R., Epureanu, B., and Heeg, J., "Reduced-Order Models in Unsteady Aerodynamics," *Proceedings of the 40th AIAA/ASME/ASCE/AHS/ASC Structures, Structural Dynamics, and Materials Conference* [CD-ROM], AIAA, Washington, D.C., 1999, pp. 229–252.

[3] Maitre, O. L., Knio, O., Najm, H., and Ghanem, R., "A Stochastic Projection Method for Fluid Flow. I: Basic Formulation," *Journal of Computational Fluids*, Vol. 173, No. 2, 2001, pp. 481–511.

[4] Xiu, D., and Karniadakis, G., "Modeling Uncertainty in Flow Simulations via Generalized Polynomial Chaos," *Journal of Computational Physics*, Vol. 187, No. 1, 2003, pp. 137–168.

[5] Millman, D., King, P. I., and Beran, P., "A Stochastic Approach for Predicting Bifurcation Of A Pitch And Plunge Airfoil," AIAA Paper 2003-3515, 2003.

[6] Millman, D. R., King, P. I., Maple, R. C., and Beran, P. S., "Predicting Uncertainty Propagation in a Highly Nonlinear System with a Stochastic Projection Method," AIAA Paper 2004-1613, 2004.

[7] Lindsley, N. J., Beran, P. S., and Pettit, C. L., "Effects of Uncertainty on Nonlinear Plate Aeroelastic Response," AIAA Paper 2002-1271, 22–25 April 2002.

[8] Pettit, C. L., "Uncertainty Quantification in Aeroelasticity: Recent Results and Research Challenges," *Journal of Aircraft*, Vol. 41, No. 5, Sept./Oct. 2004, pp. 1217–1229.

[9] Haldar, A., and Mahadevan, S., *Reliability Assessment Using Stochastic Finite Element Analysis*, Wiley, New York, 2000.

[10] Tang, D., and Dowell, E., "Effects of Angle of Attack on Nonlinear Flutter of a Delta Wing," *AIAA Journal*, Vol. 39, No. 1, 2001, pp. 15–21.

[11] Attar, P., Dowell, E., and Tang, D., "A Theoretical and Experimental Investigation of the Effects of a Steady Angle of Attack on the Nonlinear Flutter of a Delta Wing Plate Model," *Journal of Fluids and Structures*, Vol. 17, No. 2, 2003, pp. 243–259.

[12] Attar, P., Dowell, E., and Tang, D., "Modeling Aerodynamic Nonlinearities for Two Aeroelastic Configurations: Delta Wing and Flapping Flag," AIAA Paper 2003-1402, 7–10 April 2003.

[13] ANSYS, ANSYS User Manual Release 7.1, Swanson Analysis Systems, Inc., 2002.

[14] Ashley, H., and Landahl, M., *Aerodynamics of Wings and Bodies*, Dover, New York, 1965.

[15] Tang D., Henry, J., and Dowell, E., "Limit Cycle Oscillations of Delta Wing Models in Low Subsonic Flow," *AIAA Journal*, Vol. 37, No. 11, 1999, pp. 155–164.

[16] Tang D., Dowell, E., and Hall, E., "Limit Cycle Oscillations of a Cantilevered Wing in Low Subsonic Flow," *AIAA Journal*, Vol. 37, No. 3, 1999, pp. 364–371.

[17] Attar, P., Dowell, E., and White, J., "Modeling the LCO of a Delta Wing Using a High Fidelity Structural Model," AIAA Paper 2004-1402, 2004.

[18] Katz, J., and Plotkin, A., *Low-Sped Aerodynamics*, 2nd ed., University Press, Cambridge, England, U.K., 2001.

[19] Hamming, R., "Stable Predictor-Corrector Methods for Ordinary Differential Equations," *Journal of ACM*, Vol. 6, No. 1, Jan. 1959, pp. 37–47.

[20] Box, G., and Müller, M. E., "A Note on the Generation of Random Normal Deviates," *Annals of the Institute of Statistical Mathematics*, Vol. 29, No. 2, 1958, pp. 610–611.

[21] Myers, R. H., and Montgomery, D. C., *Response Surface Methodology*, Wiley, New York, 2002.

[22] Hall, K., Thomas, J. P., and Clark, W., "Computation of Unsteady Nonlinear Flows in Cascades Using a Harmonic Balance Technique," *AIAA Journal*, Vol. 40, No. 5, May 2002, pp. 879–886.

[23] Kholodar, D. B., Thomas, J. P., Dowell, E. H., and Hall, K. C., "A Parametric Study of Transonic Airfoil Flutter and Limit Cycle Oscillation Behavior," AIAA Paper 2002-1211, 2002.

[24] Thomas, J. P., Dowell, E. H., Hall, K. C., and Denegri, C. M., "Modeling Limit Cycle Oscillation Behavior of the F-16 Fighter Using Harmonic Balance Approach," AIAA Paper 2004-1696, 2004.

[25] Thomas, J. P., Dowell, E. H., and Hall, K. C., "A Harmonic Balance Approach for Modeling Three-Dimensional Nonlinear Unsteady Aerodynamics and Aeroelasticity," IMECE 2002-3252, 2002.

[26] Thomas, J. P., Dowell, E. H., and Hall, K. C., "Modeling Viscous Transonic Limit Cycle Behavior Using a Harmonic Balance Approach," *Journal of Aircraft*, Vol. 41, No. 6, Nov.–Dec. 2004, pp. 1266–1274.

[27] Beran, P., and Pettit, C., "A Direct Method for Quantifying Limit-Cycle Oscillation Response Characteristics in the Presence of Uncertainties," AIAA Paper 2004-1695, 19–22 April 2004.

This article has been cited by:

1. Sang Wu, Eli Livne. 2016. Probabilistic Aeroservoelastic Reliability Assessment Considering Control System Component Uncertainty. *AIAA Journal* **54**:8, 2507-2520. [Abstract] [Full Text] [PDF] [PDF Plus]
2. Sang Wu, Eli LivneAeroservoelastic Simulation Considering Control System Component Uncertainty . [Citation] [PDF] [PDF Plus]
3. Bret Stanford, Philip Beran. 2013. Minimum-mass panels under probabilistic aeroelastic flutter constraints. *Finite Elements in Analysis and Design* **70-71**, 15-26. [CrossRef]
4. Senthil Murugan, R. Chowdhury, S. Adhikari, M.I. Friswell. 2012. Helicopter aeroelastic analysis with spatially uncertain rotor blade properties. *Aerospace Science and Technology* **16**:1, 29-39. [CrossRef]
5. Bret Stanford, Philip Beran. 2012. Computational strategies for reliability-based structural optimization of aeroelastic limit cycle oscillations. *Structural and Multidisciplinary Optimization* **45**:1, 83-99. [CrossRef]
6. K.J. Badcock, S. Timme, S. Marques, H. Khodaparast, M. Prandina, J.E. Mottershead, A. Swift, A. Da Ronch, M.A. Woodgate. 2011. Transonic aeroelastic simulation for instability searches and uncertainty analysis. *Progress in Aerospace Sciences* **47**:5, 392-423. [CrossRef]
7. Senthil Murugan, Rajib Chowdhury, Sondipon Adhikari, Michael FriswellEffects of Spatially Uncertain Structural Properties on Helicopter Aeroelastic Response Predictions using High Dimensional Model Representation . [Citation] [PDF] [PDF Plus]
8. Senthil Murugan, Ranjan Ganguli, Dinesh Kumar Harursampath. 2011. Stochastic Aeroelastic Analysis of Composite Helicopter Rotor. *Journal of the American Helicopter Society* **56**:1, 012001. [CrossRef]
9. Sameer B. Mulani, Pankaj Joshi, Jing Li, Rakesh K. Kapania, Yung Seok Shin. 2010. Optimal Design of Unitized Structures Using Response Surface Approaches. *Journal of Aircraft* **47**:6, 1898-1906. [Citation] [PDF] [PDF Plus]
10. F. Borello, E. Cestino, G. Frulla. 2010. Structural Uncertainty Effect on Classical Wing Flutter Characteristics. *Journal of Aerospace Engineering* **23**:4, 327-338. [CrossRef]
11. Hamed Haddad Khodaparast, John E. Mottershead, Kenneth J. Badcock. 2010. Propagation of structural uncertainty to linear aeroelastic stability. *Computers & Structures* **88**:3-4, 223-236. [CrossRef]
12. S. Murugan, D. Harursampath, R. Ganguli. 2008. Material Uncertainty Propagation in Helicopter Nonlinear Aeroelastic Response and Vibratory Analysis. *AIAA Journal* **46**:9, 2332-2344. [Citation] [PDF] [PDF Plus]
13. S. Murugan, R. Ganguli, D. Harursampath. 2008. Aeroelastic Response of Composite Helicopter Rotor with Random Material Properties. *Journal of Aircraft* **45**:1, 306-322. [Citation] [PDF] [PDF Plus]